Tree Physiology 00, 1–17
https://doi.org/10.1093/treephys/tpab141

Research paper

Diverging responses of water and carbon relations during and after heat and hot drought stress in *Pinus sylvestris*

Romy Rehschuh[1,2] and Nadine K. Ruehr[1]

[1]Karlsruhe Institute of Technology, Institute of Meteorology and Climate Research-Atmospheric Environmental Research (KIT/IMK-IFU), Kreuzeckbahnstraße 19, 82467 Garmisch-Partenkirchen, Germany; [2]Corresponding author (romy.rehschuh@kit.edu; romy.rehschuh@gmail.com)

Received July 11, 2021; accepted October 22, 2021; handling Editor David Tissue

Forests are increasingly affected by heatwaves, often co-occurring with drought, with consequences for water and carbon (C) cycling. However, our ability to project tree resilience to more intense hot droughts remains limited. Here, we used single tree chambers ($n = 18$) to investigate transpiration (E), net assimilation (A_{net}), root respiration (R_{root}) and stem diameter change in Scots pine seedlings in a control treatment and during gradually intensifying heat or drought-heat stress (max. 42 °C), including recovery. Alongside this, we assessed indicators of stress impacts and recovery capacities. In the heat treatment, excessive leaf heating was mitigated via increased E, while under drought-heat, E ceased and leaf temperatures reached 46 °C. However, leaf electrolyte leakage was negligible, while light-adapted quantum yield of photosystem II (F'_v/F'_m) declined alongside A_{net} moderately in heat, but strongly in drought-heat seedlings, in which respiration exceeded C uptake. Drought-heat largely affected the hydraulic system as apparent in stem diameter shrinkage, declining relative needle water content (RWC_{Needle}) and water potential (Ψ_{Needle}) reaching −2.7 MPa, alongside a 90% decline of leaf hydraulic conductance (K_{Leaf}). Heat alone resulted in low functional impairment and all measured parameters recovered quickly. Contrary, following drought-heat, the recovery of K_{Leaf} was incomplete and stem hydraulic conductivity (K_S) was 25% lower than the control. However, F'_v/F'_m recovered and the tree net C balance reached control values 2 days post-stress, with stem increment rates accelerating during the second recovery week. This indicates a new equilibrium of C uptake and release in drought-heat seedlings independent of hydraulic impairment, which may slowly contribute to the repair of damaged tissues. In summary, Scots pine recovered rapidly following moderate heat stress, while combined with drought, hydraulic and thermal stress intensified, resulting in functional damage and slow recovery of hydraulic conductance. This incomplete hydraulic recovery could critically limit evaporative cooling capacities and C uptake under repeated heatwaves.

Keywords: electrolyte leakage, leaf hydraulic conductance, photosynthesis, recovery, root respiration, Scots pine, stem hydraulic conductivity, transpiration.

Introduction

In the past two decades, extreme summer heatwaves and drought periods, combined with high vapor pressure deficit (VPD; Grossiord et al. 2020), have been increasing in Central Europe (Ciais et al. 2005, Ionita et al. 2017, IPCC 2018). This has increased the pressure on forests, thus reducing primary productivity and enhancing hydraulic constraints, which might lead to decreased vitality and/or tree death in the long term (Anderegg et al. 2019, McDowell et al. 2020, Schuldt et al. 2020, Arend et al. 2021). Global climate change is forecast to continue and includes—besides the ecological aspect—the decline of economically important tree species (Hanewinkel et al. 2013) such as Scots pine (*Pinus sylvestris* L.). Although considered a rather drought-resistant species in Central Europe (Ellenberg and Leuschner 2010, Kunert 2020), heatwaves and drought spells are increasingly limiting its survival, causing c. 40% of the European forest mortality events (Allen et al. 2010).

Studies on the resistance of conifers to thermal stress are limited (Escandón et al. 2016). Further, few experimental studies have focused on the responses of trees to a combination of heat and drought stress (e.g., Bauweraerts et al. 2013, Bauweraerts et al. 2014, Birami et al. 2020, Kumarathunge et al. 2020, Zhao et al. 2013), and even fewer have addressed subsequent recovery trajectories (Birami et al. 2018, Ruehr et al. 2016, Ruehr et al. 2019). In general, our understanding of tree physiological recovery from combined heatwaves and drought stress is very limited (Ruehr et al. 2019), thus hindering our ability to forecast tree responses to climatic extremes. Recently, Ruehr et al. (2019) suggested that recovery trajectories depend on stress impact, indicating that physiological recovery will be slower if stress causes functional impairment and/or damage. Hence, to understand recovery trajectories, stress impacts need to be quantified properly.

High temperatures affect the water and carbon (C) relations of trees. Carbon uptake via photosynthesis is closely linked to stomatal conductance (g_s) and water loss via transpiration (E). During heat, increasing E can cool leaves if soil water is not limiting, while stomata have been found to remain at least partially open (Drake et al. 2018, Urban et al. 2017*b*). Drought stress, however, exacerbates during heatwaves as the evaporative demand increases, forcing water loss from trees. Drought-induced stomatal closure typically delays the decrease of tree-internal water potentials to critical values, but impedes transpirational leaf cooling, thus inducing higher leaf temperatures (Birami et al. 2018, Drake et al. 2018, Scherrer et al. 2011). As a result of high temperatures, photosynthetic processes might be affected by decreased activity of Rubisco activase and photosystem II, reduced CO_2 solubility and inhibited electron transport (Birami et al. 2018, Sage et al. 2008, Schrader et al. 2004, Smith and Stitt 2007, von Caemmerer and Evans 2015). Excessive leaf temperatures may further lead to cell membrane damages in leaves, typically observed via electrolyte leakage (Correia et al. 2013, Escandón et al. 2016, Saelim and Zwiazek 2000). This often involves the buildup of reactive oxygen species (Demidchik et al. 2014, Larkindale and Knight 2002), which can further impair cell membranes and proteins (O'Kane et al. 1996). In addition, drought can directly alter leaf hydraulic conductance (K_{Leaf}), i.e., the capacity of leaves to transport water. Typically, extra-xylary leave tissues are affected first and leaf xylem embolism form at higher levels of dehydration (e.g., Brodribb and Cochard 2009, Cochard et al. 2004, Johnson et al. 2009, Skelton et al. 2017). However, less information on hydraulic responses to high temperatures exists, and responses of K_{Leaf} range from no effect under extreme heat stress (Drake et al. 2018) to increases under modest temperature increments, and have been related to changes in the viscosity of water and the symplastic conductance (Sellin and Kupper 2007, Way et al. 2013).

Besides direct impacts of high temperature and drought on assimilation (A_{net}), respiratory processes are also affected (Birami et al. 2020, Gauthier et al. 2014). Root respiration (R_{root}) provides energy for maintenance and growth, necessary for root water and ion uptake (Atkin et al. 2000). However, under heat and hot drought, R_{root} has been found to decline, with reduced C availability being one of the reasons (Birami et al. 2020). Yet, reduced C uptake can also limit aboveground respiration and growth. So far, the knowledge of growth processes in response to heatwaves remains elusive, and should be evaluated in combination with water limitation (Ruehr et al. 2016). Under both, heat and drought-heat, stem diameter growth has been shown to cease, particularly under water limitation (Bauweraerts et al. 2014, Ruehr et al. 2016). Large proportions (>90%) of stem diameter fluctuations result from swelling or shrinkage of the elastic bark, providing information on tree water dynamics (Zweifel et al. 2000, Zweifel and Häsler 2000). Measurements of tree water status in combination with gas exchange could reveal important insights on tree physiological mechanisms and processes.

In addition to evaluating stress effects, process understanding of post-stress-recovery dynamics are crucial for estimating the resilience of trees and forests to climate change. This can provide further information in order to adapt forest management in the long term. Stress impacts may leave physiological functions impaired for weeks up to years post-stress (Anderegg et al. 2015, Rehschuh et al. 2020, Ruehr et al. 2019, Schuldt et al. 2020). Depending on stress severity (Ruehr et al. 2019), this includes the persistent reduction of gas exchange (Birami et al. 2018, Duarte et al. 2016, Rehschuh et al. 2020, Ruehr et al. 2016), often associated with the impairment of the photosynthetic apparatus (Ameye et al. 2012, Birami et al. 2018) and the lack of full recovery of the hydraulic system (Brodribb et al. 2010, Rehschuh et al. 2020). Further, stem increment rates have been shown to remain low post-stress (Anderegg et al. 2015, Rehschuh et al. 2017), potentially triggered by the stress-induced reduction of leaf area and C reserves (Galiano et al. 2011). Therefore, the rapid recovery of net C gain may play an important role during recovery, as it provides energy and C skeletons for repair and regrowth processes.

Here, we tested the impacts of a prolonged, moderate heatwave on the hydraulic and metabolic recovery of well-watered and drought-treated *Pinus sylvestris* seedlings. For this, seedlings were placed in individual gas exchange chambers, while continuously measuring above- and belowground CO_2 and H_2O dynamics, as well as stem diameter change. Further, parameters related to functional integrity of leaves such as the maximum light-adapted quantum yield of photosystem II (F'_v/F'_m) and electrolyte leakage were investigated. The following hypotheses were tested:

(i) Low transpiration rates during heatwaves result in higher thermal stress that causes tissue damage.
(ii) Metabolic and hydraulic recovery will be fast if stress does not result in functional impairment and/or damage.

(iii) Stress-induced impacts on hydraulic properties will be directly linked to the recovery of the tree C balance and stem growth.

Materials and methods

Plant material and growth conditions

Three-year-old *Pinus sylvestris* seedlings originating from a tree nursery in Middle Franconia (provenance 85,115), Germany, were potted in round pots (18 cm in height, 22 cm in diameter) in March 2018. To assess the whole-tree C balance (net C uptake = net photosynthesis − respiration) we used a C-free potting substrate, i.e., a mixture of fine quartz sand (0.1–1.2 mm), medium-grained sand (1–2.5 mm) gravel (3–5.6 mm), and vermiculite in a relation of 2:2:1:2. The substrate was enriched with 12 g of slow-release fertilizer (Osmocote® Exact Standard 5-6 M fertilizer 15–9-12 + 2MgO + TE, ICL Specialty Fertilizers, The Netherlands) per pot and liquid fertilizer (Compo® Complete, 6 + 4 + 6(+2) NPK(MgO), Hornbach, Germany) added monthly during the growing season. During the entire adjustment and experimental period, seedlings were kept in a scientific greenhouse facility in Garmisch-Partenkirchen, Germany (708 m above sea level (a.s.l.), 47°28′32.9″N, 11°3′44.2″E) with highly UV-transmissive glass. Additionally, growth lamps (T-agro 400 W, Philips, Hamburg, Germany) were used to supplement outside light. Photosynthetic active radiation (PAR) inside the greenhouse was measured continuously (PQS 1, Kipp & Zonen, Delft, The Netherlands), reaching daytime averages of 350–550 μmol m^{-2} s^{-1}.

Drought and heatwave conditions

Seedlings were randomly assigned to a well-watered control, a heat and a combined drought-heat treatment, in which we assessed stress and recovery trajectories (see experimental timeline Figure S1 available as Supplementary data at *Tree Physiology* Online). After needle elongation was completed (2 August 2018), seedlings assigned to the drought-heat treatment were subjected to 1.5 months of reduced irrigation, keeping the soil volumetric water content (VWC) close to 10% (EC5, Meter Group, USA). The VWC was adjusted automatically by a drip irrigation system (Rain Bird, Azusa, CA, USA), and was close to field capacity at 22% in the control treatment. Throughout this initial drought period before the heatwave was initiated, air temperature (T_{air}) and relative humidity (RH; CS215, Campbell Scientific, Logan, UT, USA) were maintained constant (CC600, RAM Regel- und Messtechnische Apparate GmbH, Herrsching, Germany) between well-watered and drought-treated seedlings (daytime: T_{air}: 22.9 ± 0.1 °C; RH: 71.6 ± 0.5%; nighttime: T_{air}: 17.4 ± 0.0 °C; RH: 81.8 ± 0.8%).

We started the main experiment in the tree gas exchange chambers (see below) on 18 September 2018, and kept the daylight length at 16 h to mimic summer conditions throughout the experiment. To adjust the environmental conditions in the stress treatments to previously observed hot drought events, we analyzed meteorological data (T_{air}, RH, VPD) from the Deutscher Wetterdienst in Weißenburg-Emetzheim, Franconia, Germany (435 m a.s.l., N49°1′38.28″ E10°58′55.2″). In this area, Scots pine dieback has been observed recently (Gößwein et al. 2017, Walentowski et al. 2017). As we found the period from 7–13 August 2003 to reveal the most intense summer extremes (Figure S2 available as Supplementary data at *Tree Physiology* Online), we based the climatic conditions during our experimental heatwave on these data. The heatwave was applied after the seedlings had been placed in individual tree chambers to automatically monitor gas exchange (see subsection below) and a 5-day acclimation phase (daytime T_{air}: 26 °C on average). During the 20-day heatwave, we stepwise increased daytime T_{air} in the stress treatments (30 °C, 33 °C, 35 °C, 38 °C and 40/41 °C period). Alongside, VPD increased concurrently to a maximum of 6 kPa in the drought-heat treatment, but remained lower (max. c. 4 kPa) in the heat treatment due to larger transpiration rates affecting air humidity inside the chambers (Figure 1a and b). T_{air} was maintained at the targeted maximum for at least 6 h per day, while in the control treatment T_{air} was on average 26 °C. Soil temperatures (T_{soil}) were not actively controlled, hence temperatures followed largely the daily amplitude of T_{air}, but at a lower intensity (Figure 1c). Because we were technically limited in our temperature control of the tree chambers during nighttime, T_{air} and T_{soil} averaged at 20 °C in all treatments. As shown from analyses of previous heatwaves in Central Europe, minimum temperatures during nighttime typically increase less than maximum temperatures during daytime (De Boeck et al. 2010).

In the control treatment, the VWC was maintained close to field capacity by watering 4× daily c. 75 ml, respectively (Figure 1d). A similar VWC was achieved in the heat treatment, while the amount had to be increased slightly due to higher transpiration rates. In the drought-heat treatment, seedlings were irrigated 2× daily during the first 5 days of acclimation (c. 50 ml, respectively) and once at 5 a.m. during the heat stress period (70 ml), while the water supply was further steadily reduced.

To analyze recovery processes, seedlings were rewatered to field capacity at 5 a.m. on 13 October 2018. T_{air} and VPD were set to control conditions and daylight length was maintained at 16 h (Figure 1a–d). Note that 2 days after stress release, a $^{13}CO_2$ pulse-labeling experiment was conducted to follow the allocation of recent C to pools and respiration following stress release (see Rehschuh et al. 2021).

Tree gas exchange chambers

For continuous monitoring of above- and belowground gas exchange (H_2O and CO_2) during the drought and heat period and the recovery phase, we randomly selected 12 well-watered seedlings that were either assigned to a control treatment (n = 6) or a heat treatment (n = 6) and drought-treated seedlings that were assigned to a drought-heat treatment (n = 6). Each of the 18 seedlings was placed in an individual tree chamber within the greenhouse compartment (Figure S3 available as Supplementary data at *Tree Physiology* Online). Seedlings used in the control, heat and drought-heat treatment were on average 57.3 ± 1.8 cm (±SE), 57.5 ± 1.9 cm and 58.1 ± 3.6 cm in height, and had a stem diameter of 16.4 ± 0.6 mm, 15.9 ± 0.5 mm and 14.9 ± 0.4 mm, respectively. The tree chambers were divided into a translucent temperature-controlled shoot compartment, which was gas-tightly sealed from an opaque root compartment (see Figure S3 available as Supplementary data at *Tree Physiology* Online; for further details on materials and technical operation of the chamber system see Birami et al. (2020) and Rehschuh et al. (2021)). T_{air} was predefined for the different treatments and days and regulated within each shoot compartment separately by fast-response thermocouples (5SC-TTTI-36-2 M, Newport Electronics GmbH, Deckenpfronn, Germany) and based on a water-cooling principle. Photosynthetic active radiation was recorded per chamber by photodiodes (G1118, Hamamatsu Photonics, Hamamatsu, Japan), calibrated in advance with a PAR sensor (PQS 1, Kipp & Zonen). T_{soil} and moisture were continuously logged (TS 107, Campbell Scientific, Inc. USA and EC 5, Meter Group, USA, respectively), and data recorded in 10 min intervals (CR1000, Campbell Scientific, Inc. USA). In addition, stem diameter change was measured half-hourly by dendrometers (DD-S, Ecomatik, Dachau, Germany), attached to each stem at ~5–10 cm above the soil surface. Increases in daily stem diameter were interpreted as growth (i.e., cell division and/or cell elongation). Directly after rewatering, we excluded a rehydration period of 6 days, i.e., until the stem diameter reached the same width as before stress.

Gas exchange measurements and calculations

Above- and belowground chamber compartments were constantly supplied with air (Air_{supply}) from an oil-free screw compressor by adding a predefined CO_2 (c. 430 p.p.m.) and H_2O concentration (8 mmol during the adjustment and recovery period; 4 mmol during the stress period). Each of the 20 shoot and root compartments received c. 13 l min^{-1} and 3 l min^{-1} of air flow, respectively.

Firstly, absolute [CO_2] and [H_2O] of Air_{supply} and sample air (Air_{sample}) were quantified by a gas analyzer (Li-840, LI-COR, Lincoln, NE, USA). Subsequently, a differential gas analyzer determined the differences between Air_{supply} and Air_{sample} (Li-7000, LI-COR). To correct for any fluctuations in [CO_2] and [H_2O] not caused by plant gas exchange, we additionally measured two empty chambers of the same design, containing no tree but each one pot with the same C-free substrate. Small differences between Air_{supply} and Air_{sample} were detected with on average 1.3 ± 0.01 μmol CO_2 mol^{-1} and 0.1 ± 0.003 mmol H_2O mol^{-1} in shoot and 3.9 ± 0.03 μmol CO_2 mol^{-1} in root compartments. The respective offsets were removed from the data accordingly before fluxes were calculated.

Each compartment was measured once every 2 h for c. 80 s and data were logged every 10 s. The following equations were used to calculate gas exchange fluxes: transpiration (E) in mol H_2O m^{-2} s^{-1} was calculated as follows:

$$E = \frac{\dot{m}\ \left(W_{sample} - W_{supply}\right)}{area_{needle}\left(1 - W_{sample}\right)}, \quad (1)$$

where $\dot{m}$ is air mass flow (mol s^{-1}), W_{supply} is [H_2O] in Air_{supply}, and W_{sample} is [H_2O] in Air_{sample}, $area_{needle}$ is the total needle area per seedling in m^2.

Stomatal conductance g_s in mmol m^{-2} s^{-1} was calculated accordingly:

$$g_s = \frac{E\left(1000 - \frac{W_{needle}+W_{sample}}{2}\right)}{W_{needle} - W_{sample}}, \quad (2)$$

where W_{needle} is the needle H_2O vapor concentration, which was deduced from saturated vapor pressure (kPa) at the prevailing T_{air} (°C) and atmospheric pressure p (kPa). This method of determining g_s assumes well mixed air within the shoot compartment and therefore, neglects the boundary layer conductance.

The belowground flux measured here was regarded as root respiration (R_{root}) since we used C-free potting substrate and corrected for potential not root-derived fluxes. Net assimilation (A_{net}), shoot dark respiration ($R_{shoot\ night}$) and R_{root} in μmol s^{-1} were calculated by the equation for CO_2 fluxes:

$$CO_2\ flux = (-\dot{m}\cdot\Delta C) - \left(E\cdot C_{sample}\right), \quad (3)$$

where ΔC is the difference between [CO_2] of Air_{supply} and Air_{sample}, and C_{sample} is [CO_2] of Air_{sample}. E was included to correct for dilution by transpiration. Further, leaf-level A_{net} in μmol m^{-2} s^{-1} was derived from total needle area, and tissue-specific R_{root} in μmol g^{-1} s^{-1} dry weight from root biomass. Whole-tree daily net C uptake (in mg C day^{-1} tree^{-1}) was calculated from cumulative hourly fluxes per day and tree by subtracting daily C loss ($R_{shoot\ night}$ and R_{root} both in μmol day^{-1} tree^{-1}) from daily C uptake (A_{net} in μmol day^{-1} tree^{-1}):

$$Net\ C\ uptake = A_{net} - \left(R_{shoot\ night} + R_{root}\right). \quad (4)$$

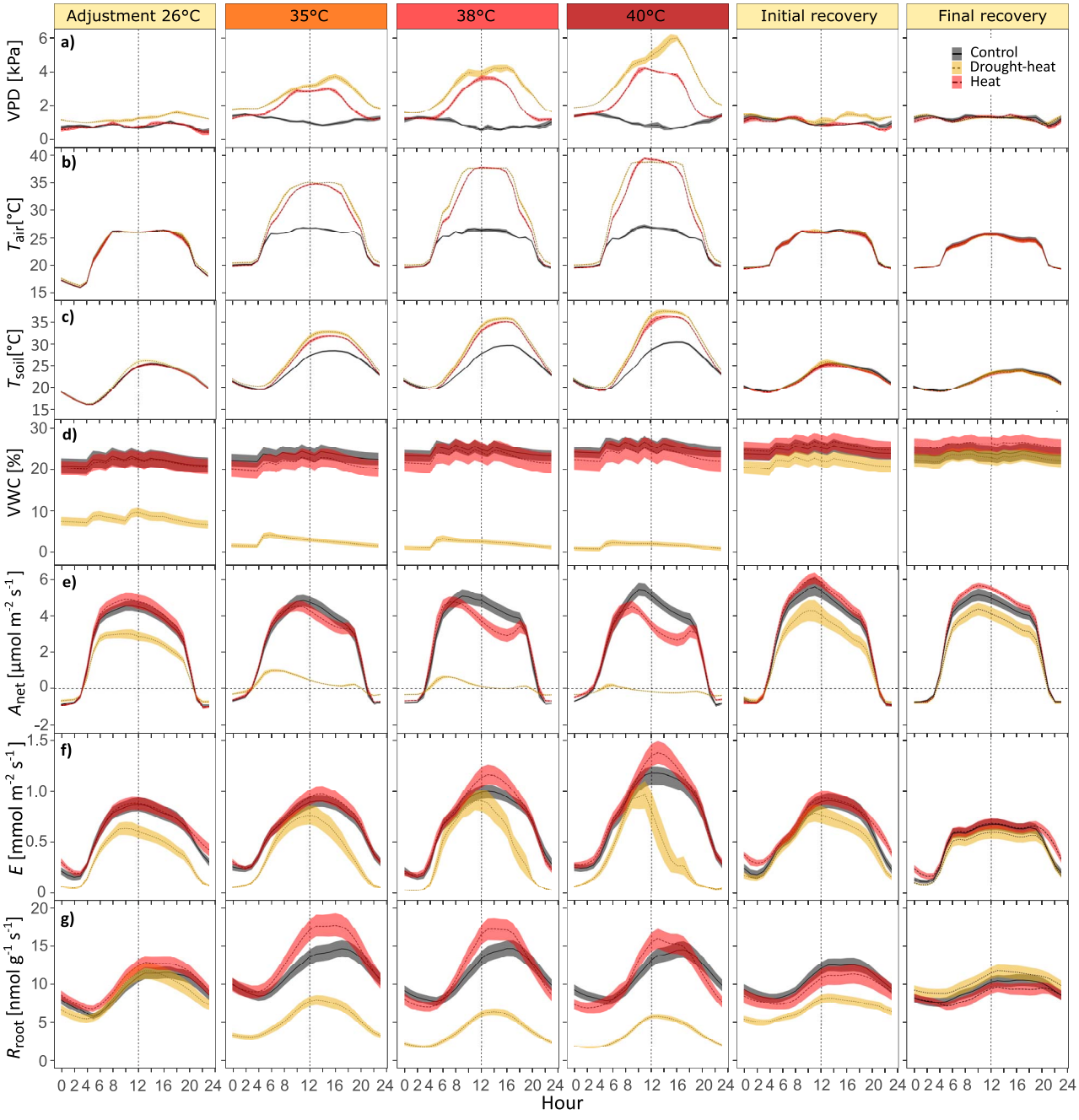

Figure 1. Diurnal dynamics of treatment-averaged hourly (a) vapor pressure deficit (VPD), (b) air temperature (T_{air}), (c) soil temperature (T_{soil}), (d) soil volumetric water content (VWC), (e) net assimilation (A_{net}), (f) transpiration (E) and (g) root respiration (R_{root}) for different periods. Before heat stress, during adjustment (26 °C, 4 days), temperature increments (35 °C, 7 days; 38 °C, 3 days; and 40 °C, 4 days), the initial (26 °C, Day 28–30) and final recovery period (26 °C, Day 40–42). Daytime length was 16 h (4:30–20:30 CET). Shown are treatment averages and shaded areas are ±SE (n = 6 per treatment).

Leaf temperature

To assess temperature and indirect drought effects, we measured leaf temperature (n = 6 per treatment) between 1 p.m. and 2 p.m. using an infrared camera (PI 450, Optris, Germany). Leaf temperature was evaluated about weekly during the stress period, and twice during the recovery phase (initial and final recovery). Mean and maximum leaf temperatures were determined from images using the manufacturer's software. For this, we corrected for background radiation using T_{air} during measurements and set emissivity to 0.97.

Maximum light-adapted quantum yield of photosystem II

We measured maximum light-adapted quantum yield of photosystem II (F'_v/F'_m) using a portable leaf-gas exchange system (Li-6400XT, LI-COR Inc.,), supplemented with a fluorescence head (6400-40 Leaf Chamber Fluorometer). Measurements

(n = 6 per treatment) were conducted between 9 a.m. and 1 p.m. about 2 weeks before placing the initially drought-treated seedlings in the tree chambers, as well as later during the heatwave and recovery phase, coordinated with leaf temperature measurements. For this, we clamped needles into the leaf cuvette, covering its area completely (2 cm^2), but avoiding overlapping of needles as much as possible. We used predetermined saturated light conditions of 1200 μmol m^{-2} s^{-1} photosynthetic photon flux density and a reference [CO_2] of 400 p.p.m.. Leaf temperature, RH and VPD were kept constant during measurements, and averaged 26 °C, 52% and 1.5 kPa in the control and 29 °C, 37% and 3 kPa in the heat and drought-heat treatment.

Electrolyte leakage

To assess cell membrane stability, we quantified electrolyte leakage of needles following Mena-Petite et al. (2003). Sampling of 10 needle fascicles on five seedlings per treatment was done in coordination with leaf temperature measurements, between 10 a.m. and 12 a.m. The samples were immediately wrapped in moist paper towels and subsequently washed in a Petri dish filled with deionized water to remove solutes from needle surfaces. Excess water was removed and needles were cut into segments of c. 1 cm length, excluding the needle sheath. The needle segments were weighed and transferred to falcon tubes (Isolab, Laborgeräte GmbH, Eschau, Germany) with 20 ml of distilled water of known electrical conductivity (EC_{dist}). Electrical conductivity was determined with a conductivity electrode (1480–90 Cole-Palmer Instruments; Chicago, L., USA). Subsequently, falcon tubes were placed inside a desiccator. To facilitate electrolyte leakage, a vacuum was created by withdrawing air. Samples were kept in the dark for 24 h at room temperature. Then, samples were shaken and EC_{final} was measured. Subsequently, samples were heated to 100 °C for 10 min to destroy all living cells and maximize leakage. After samples were cooled to room temperature, EC_{total} was determined. Twenty-four hour electrolyte leakage was then calculated as follows:

$$EC = \frac{EC_{final} - EC_{dist}}{EC_{total} - EC_{dist}} \cdot 100, \quad (5)$$

which was then related to needle weight and expressed relative to control seedlings.

Leaf hydraulic conductance (K_{Leaf})

K_{Leaf} was measured between 10 a.m. and 12 a.m. on five to six seedlings per treatment, coordinated with F'_v/F'_m measurements. We adjusted the evaporative flux method used by Sack and Scoffoni (2012) to measure single needles of seedlings as follows. Needle fascicles were detached from branches under water and placed with their base in Eppendorf tubes filled with distilled and filtered water (0.22 μm pore size). After an adjustment time of c. 20 min in ventilated air to enhance E under constant light conditions (800–1000 μmol m^{-2} s^{-1} PAR), E of a single needle fascicle was measured using a portable leaf-gas exchange system (Li-6400XT, LI-COR Inc.,) equipped with a light source (6400-40 Leaf Chamber Fluorometer) under saturated light conditions of 1200 μmol m^{-2} s^{-1} PAR and [CO_2] of 400 p.p.m. until stable conditions were reached. Temperature and RH during acclimation and measurement corresponded to conditions inside the tree chambers per treatment and measurement time point. After measuring E, the same needle fascicles were placed in nontransparent plastic bags to equilibrate for 20 min whereupon Ψ_{Needle} was determined using a Scholander pressure chamber (Model 1000, PMS Instruments, Albany, OR, USA). The projected needle area (A_{Leaf}) of the enclosed needle segments was determined using a leaf area meter (Li-3,100, LI-COR Inc.,). K_{Leaf} in mmol m^{-2} s^{-1} MPa^{-1} was then calculated as follows:

$$K_{Leaf} = \frac{E}{\Psi_{Needle} \cdot A_{Leaf}}. \quad (6)$$

Needle water potential (Ψ_{Needle}) and relative needle water content (RWC_{Needle})

To assess tree water status, we measured predawn and midday Ψ_{Needle} of mature needles of six seedlings per treatment using a Scholander pressure chamber (Model 1000, PMS Instruments). We report daily minimum Ψ_{Needle} since predawn Ψ_{Needle} was measured before the automatic irrigation and hence sometimes slightly lower than midday Ψ_{Needle}. Measurements of Ψ_{Needle} were coordinated with RWC_{Needle} measurements. For this, we sampled two needle fascicles per seedling (n = 6 per treatment), placed them in a plastic bag to avoid evaporation and immediately determined fresh weight (W_{fresh}). After soaking them in purified water at room temperature for 48 h (as predetermined from saturation curves), turgid weight (W_{turgid}) was measured, then needles placed in an oven at 70 °C for 48 h, and consequently dry weight (W_{DW}) determined. RWC_{Needle} was calculated as follows:

$$RWC_{Needle}\ (\%) = 100 \cdot \frac{W_{fresh} - W_{DW}}{W_{turgid} - W_{DW}}. \quad (7)$$

Biomass and needle area

We sampled the biomass of the seedlings (n = 6 per treatment) at the end of the experiment and took a subsample to determine stem hydraulic conductivity (see below). Biomass was then separated into leaf, root, branch and stem tissues and oven-dried for 48 h at 70 °C to determine DW.

Leaf area of each tree was derived from leaf biomass and predetermined specific leaf area (gDW cm^{-2}). On a subsample of fresh needles, specific leaf area was measured using an area meter (Li-3,100, LI-COR Inc.,), and its dry mass determined. Total leaf area per tree was then calculated via this leaf area index.

Stem xylem hydraulic conductivity (K_S)

A part of each stem was wrapped in cling film and frozen immediately in plastic bags at −18 °C to determine K_S (n = 6 per treatment) by applying the pressure-flow method (Sperry and Tyree 1988), as described more detailed in Rehschuh et al. (2020). In short, frozen samples were thawed in distilled water, cut back underwater with sharp instruments, and the bark was peeled off. Samples were fixed in a fivefold valve (Luer-lock system; neoLab Migge Laborbedarf-Vertriebs GmbH, Heidelberg, Germany), and exposed to a pressure of 0.004 MPa of water flow to determine in situ degree of embolism. A mass flow meter (mini-CORI-FLOW M13, Bronkhorst, Montigny les Cormeilles, France) served to measure the flow rate of each stem segment individually. By considering the xylem cross-sectional area and sample length, we then determined K_S. Note that we observed a small ring of inactive xylem area in all samples. Hence, we avoided saturation of samples via flushing to not yield unrealistically high K_S due to refilling of older, already dysfunctional conduits. To facilitate comparison of stress-induced impacts on K_s and K_{Leaf} at the end of the experimental period, we additionally provide K_s and K_{Leaf} relative to the respective mean of control seedlings.

Statistical data analysis

Gas exchange data were quality-checked per chamber, and outliers identified separately for day- and nighttime measurements based on the widely applied boxplot approach. For this, values outside 1.5 times the interquartile range above the upper and below the lower quartile were removed. Between Day 32 and 34, daily net C uptake was calculated from linear interpolation due to data unavailability because of technical constraints. For diurnal progression analysis of gas exchange data and depiction of environmental variables, we hourly averaged data from several key experimental periods (adjustment period at 26 °C, temperature stages (35 °C, 38 °C and 40 °C), initial stable and final recovery period).

Data processing and statistical analyses were performed in 'R' version 3.6.1 (R Development Core Team 2019). Differences between treatments (significant if $P < 0.05$) were determined per measurement campaign for discretely measured parameters (e.g., leaf temperature, F'_v/F'_m, K_{Leaf}) by applying the Kruskal–Wallis followed by the Bonferroni post-hoc test, therefore accounting for small sample sizes.

Treatment effects on continuous data (gas exchange measurements, net C uptake) were assessed by applying linear-mixed effects models (lme; lmerTest package; Kuznetsova et al. 2017). Treatment and time period were assigned as fixed effect and chamber as random factor. Time periods included the adjustment period, the different temperature steps, initial and final recovery. For diurnal measurements, we further considered day- and nighttime. We selected the model with the lowest Akaike's information criterion corrected for small sample size (Burnham and Anderson 2002), i.e., the most parsimonious model. Further, we used the post-hoc Tukey's multiple comparisons test of means for the determination of differences between treatments (package emmeans; Lenth et al. 2020) and provide Tukey's HSD.

Further, we analyzed leaf temperature dependencies of A_{net}, F'_v/F'_m, electrolyte leakage and K_{Leaf}, and relationships of Ψ_{Needle} with gas exchange parameters (A_{net}, net C uptake, E). Additionally, we tested for the relationships of net C uptake with stem diameter change during stress and recovery separately. Where applicable, we fitted polynomial or sigmoidal functions for better visualization of relationships. Fitted curves for stem diameter change in relation to C uptake during recovery were analyzed for significant differences between treatments by comparing their coefficients.

Results

Drought stress was initiated after needle growth was completed and no significant differences between treatments in needle biomass and area were found (Figure S4 available as Supplementary data at *Tree Physiology* Online). However, a modest effect of the prolonged drought became visible as the root:shoot ratio (−25%), root (−23%) and woody biomass (−15%) tended to be lower than in control seedlings.

Tree gas exchange, net C uptake and stem diameter change during stress and recovery

During daytime, increases in T_{air} enhanced VPD (Figure 1a and b). This increase in VPD was larger in the drought-heat treatment due to lower transpiration rates, which reduced the RH inside the tree chambers. Nighttime temperatures, however, did not differ largely between treatments, and were maintained close to 20 °C.

The effects of 6 weeks of moderate drought stress became visible in the diurnal course of E and A_{net}, which remained below control seedlings already before the heatwave was initiated (Tukey's HSD, $P < 0.01$, see Table S2 available as Supplementary data at *Tree Physiology* Online for P-values; Figure 1e and f). With increasing temperatures and VPD, E in drought-heat seedlings approximated control values during the morning hours, but decreased dramatically in the course of the day, intensified with stress progression (Tukey's HSD, $P < 0.05$ for 38 °C and $P < 0.001$ for 40 °C period). In heat seedlings, E increased with a rise in T_{air} and VPD, despite declining g_s (Figure S5b available as Supplementary data at *Tree Physiology* Online). This was reflected in diurnal dynamics of A_{net}, which decreased to about 70% of control values during periods of high T_{air} and VPD (Tukey's HSD, $P < 0.001$ for 40 °C period; Figure 1a and b) between 10 a.m. and 4 p.m., followed by a slight increase later (Figure 1e). Under combined drought and heat stress, we found a strong decline in A_{net}, which was reflected in partial to full stomatal closure (Figure S6 available as Supplementary data at *Tree Physiology* Online), with g_s

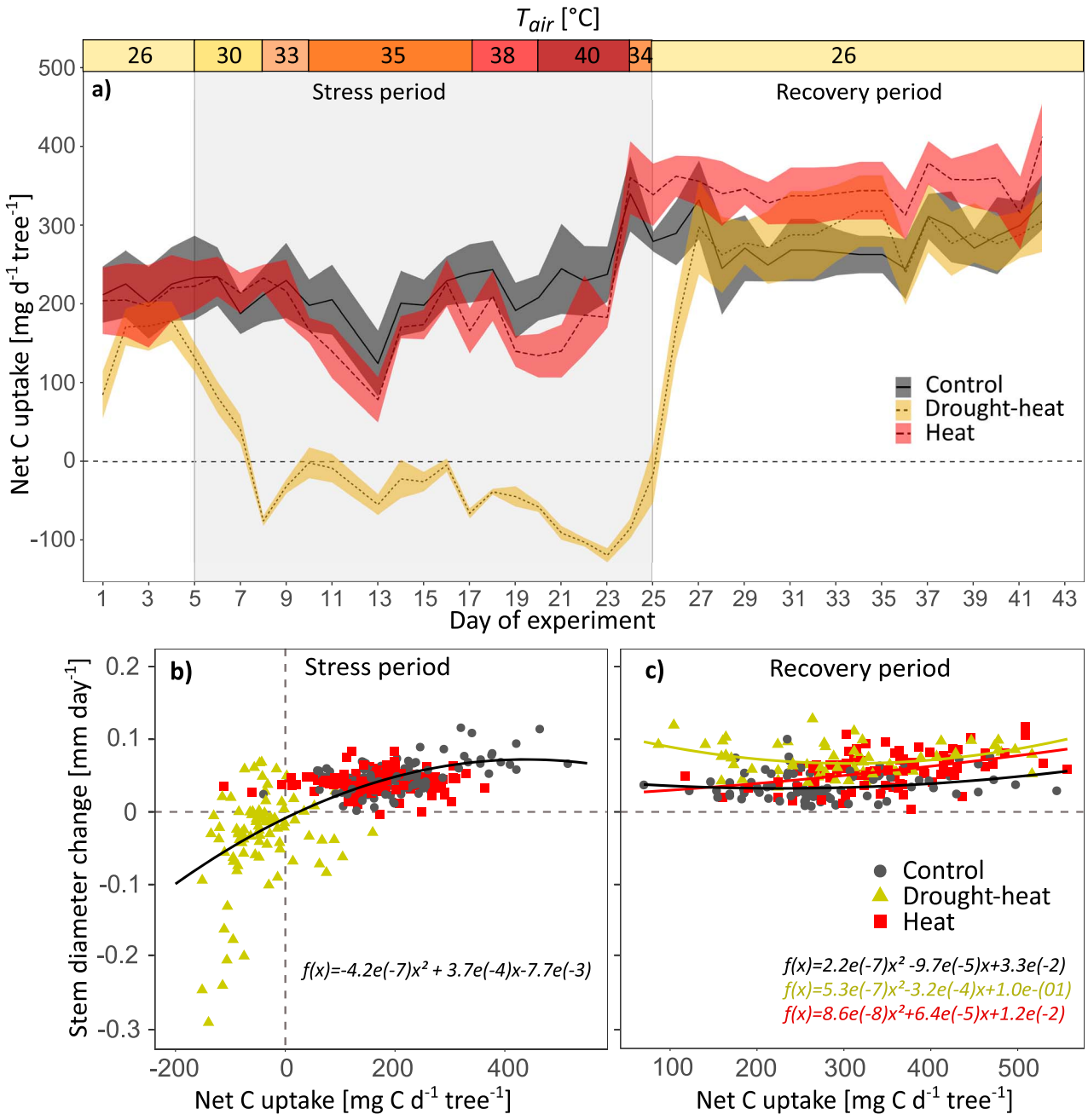

Figure 2. Daily net carbon (C) uptake of Scots pine seedlings during the entire experiment (a) and in relation to stem diameter change during stress (b) and recovery (c). The daily net C uptake per seedling was derived by summing hourly means of C uptake by photosynthesis minus C release by shoot and root respiration. In (a), the shaded areas show ±SE (n = 6). Mean daytime air temperature (T_{air}) is given for the stress treatments, while control seedlings were at 26–28 °C. In (b) and (c) diurnal stem diameter changes per seedling and treatment are shown. Negative stem diameter change was caused by stem shrinkage due to tree water deficit. The rehydration period after drought-heat release (6 days), i.e., until stem diameter width reached initial values before tree water deficit, was excluded from data analyses of the recovery period.

being lower at the same VPD and T_{air} compared with the heat treatment (Figure S5 available as Supplementary data at *Tree Physiology* Online).

R_{root} largely followed diurnal soil temperature patterns (Figure 1c,g, Figure S7 available as Supplementary data at *Tree Physiology* Online). Over the 20-day heat period, R_{root} initially increased in the heat treatment, but when 40 °C prevailed, the difference to control seedlings diminished, indicating some kind of adjustment. In the drought-heat treatment, R_{root} declined with an increase in T_{soil} and was about threefold lower than in the control during the 35 °C–40 °C period (Tukey's HSD, $P < 0.01$; Figure 1g).

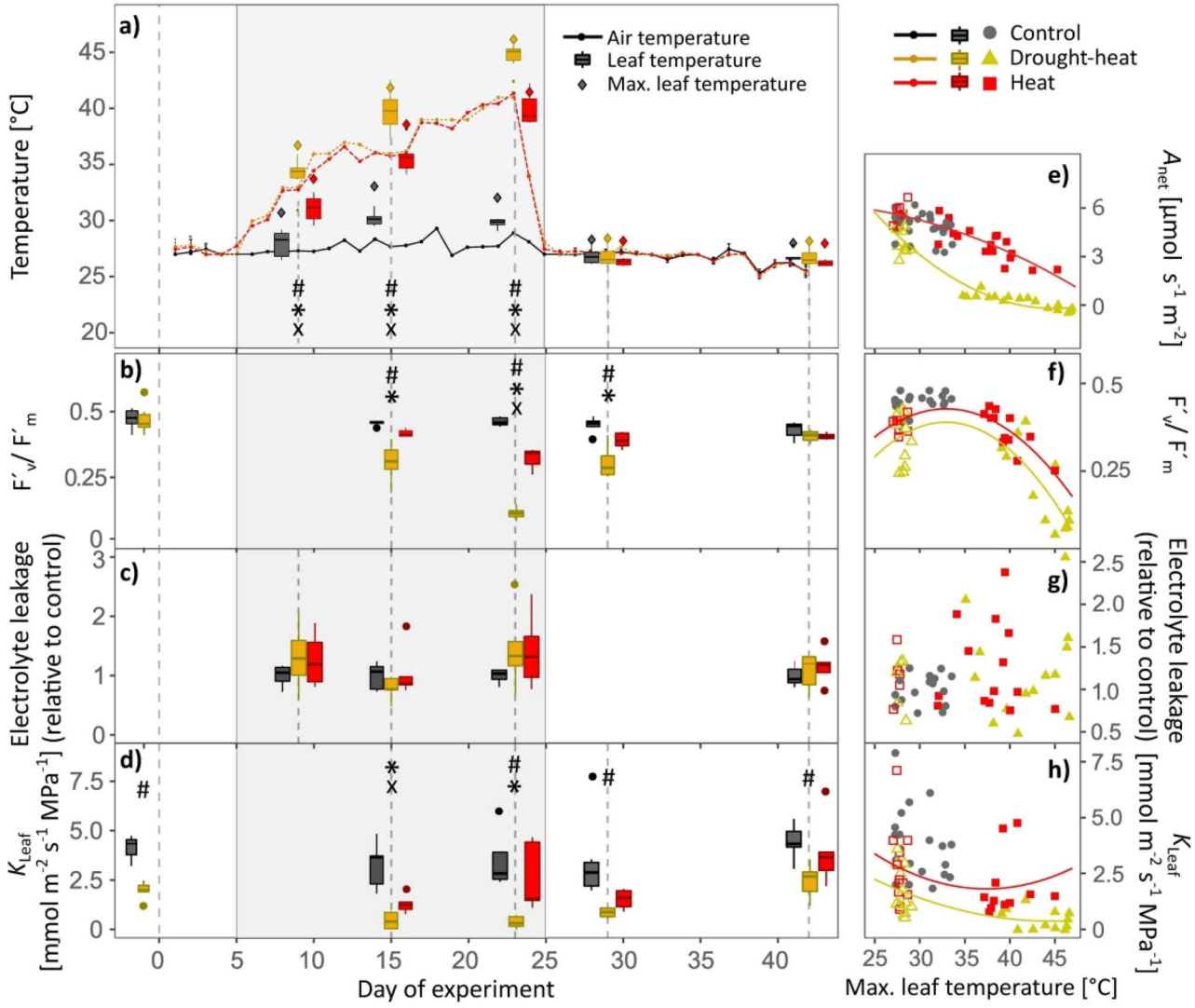

Figure 3. Dynamics of air and leaf temperature and stress indicators during the experimental phase in Scots pine seedlings. Shown are (a) air temperature, mean and maximum leaf temperature, (b) maximum light-adapted quantum yield of photosystem II (F'_v/F'_m), (c) electrolyte leakage and (d) leaf hydraulic conductance (K_{Leaf}) during stress progression and recovery (n = 5–6 per treatment). In (e–h) the relationships of A_{net}, F'_v/F'_m, electrolyte leakage and K_{Leaf} with maximum leaf temperature during stress and recovery are shown per seedling and treatment. The gray boxes represent the stress period. Symbols indicate significant differences ($P < 0.05$) between treatments per sampling campaign (Kruskal–Wallis and Bonferroni post-hoc test) as follows: drought-heat vs control (#), heat vs control (x) and drought-heat vs heat (*). Note that data before Day 0 are for measurements 2 weeks before the chamber experiment started and that drought-heat seedlings were long-term drought-stressed for 1.5 months. Open symbols in (e–h) indicate measurements during the recovery period. Polynomial curves were fitted for the drought-heat and heat treatment if applicable (for functions see Table S1 available as Supplementary data at *Tree Physiology* Online).

The daily tree net C uptake appeared to be moderately affected in the heat treatment, particularly when T_{air} reached >38 °C and VPD rose >3 kPa (Figure 2a, see also Figure S8 available as Supplementary data at *Tree Physiology* Online for daily means of A_{net}, $R_{shoot\ night}$ and R_{root} per tree). The effect on the C balance was more apparent when heat was combined with drought. Although net C uptake and stem growth (Figure 2a and b) continued under heat, net C uptake decreased in drought-heat seedlings, resulting in a negative C balance (Tukey's HSD, $P < 0.001$ compared with heat and control). This was reflected in stem growth cessation and phloem shrinkage due to water deficits (Figure 2b).

Following stress release on Day 25 of continuous gas exchange measurements, we observed a fast response of E and net C uptake (Tukey's HSD, $P > 0.1$ for stress treatments compared with control; Table S2 available as Supplementary data at *Tree Physiology* Online). In the heat treatment, net C uptake tended to exceed that of the control seedlings by c. 10%, also reflected in higher daily stem increment rates ($P > 0.05$; Figure 2c). Surprisingly, net C uptake in

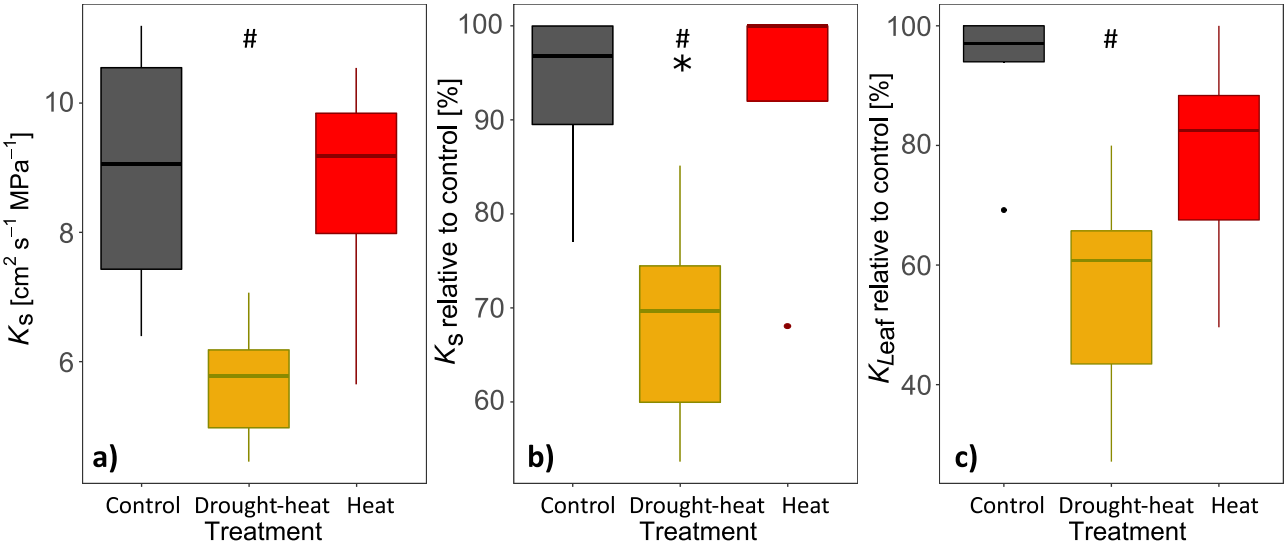

Figure 4. Treatment-specific stem hydraulic conductivity (K_S) and leaf hydraulic conductance (K_{Leaf}) 18 days after stress release. Shown are boxplots per treatment of absolute K_S (a), as well as K_S (b) and K_{Leaf} (c) relative to the average of the control treatment (n = 5–6). Symbols indicate significant differences ($P < 0.05$) between drought-heat and control (#), and between drought-heat and heat (*) (Kruskal–Wallis & Bonferroni post-hoc test).

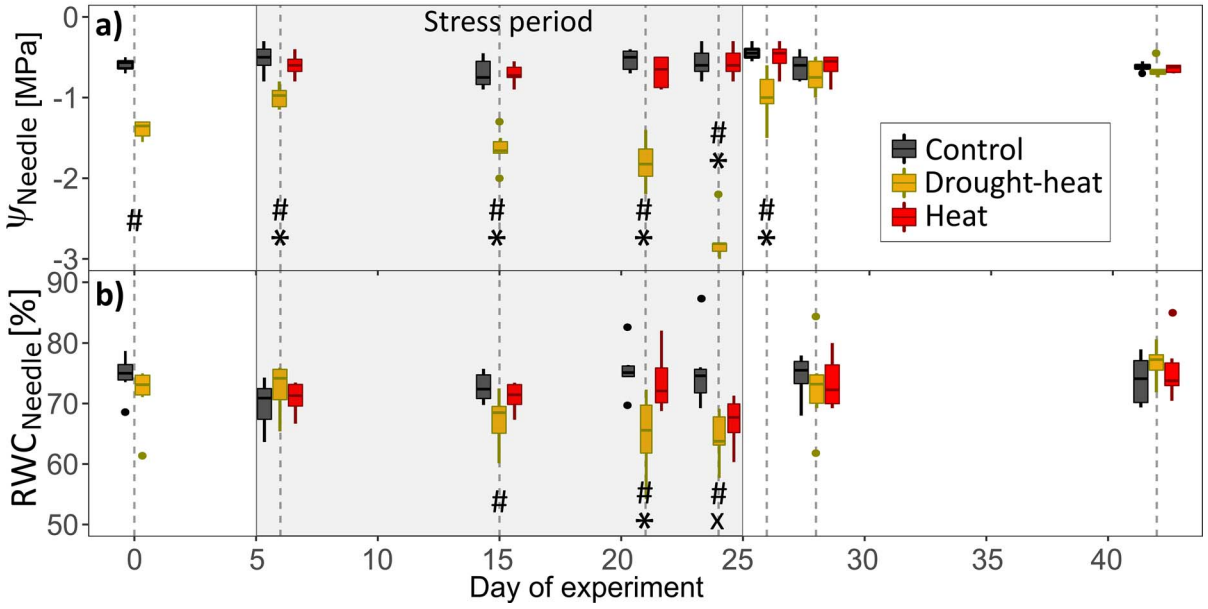

Figure 5. Treatment-specific dynamics of (a) needle water potential (Ψ_{Needle}, n = 6) and (b) relative needle water content (RWC_{Needle}, n = 6) during stress and recovery. The gray boxes represent the stress period. Symbols indicate significant differences ($P < 0.05$) between treatments per measurement campaign (Kruskal–Wallis and Bonferroni post-hoc test) as follows: drought-heat vs control (#), heat vs control (x), and drought-heat vs heat (*). Note that drought-heat seedlings were long-term drought-stressed for 1.5 months before the start of the main experiment (Day 1).

drought-heat treated seedlings reached control values within 2 days, whereas A_{net} remained c. 20% below control rates (Tukey's HSD, $P < 0.05$ for initial and $P = 0.08$ for final recovery period; Figure 1e). The fast recovery of tree net C uptake can be explained by an initially slow recovery of R_{root} (Tukey's HSD, $P < 0.05$ compared with control, Figure 1g) and a tendency for a lower root:shoot ratio (i.e., R_{root} at the tree level did not fully recover, see Figure S8 available as Supplementary data at *Tree Physiology* Online). Alongside, stems rehydrated to before-stress diameter width slowly during 6 days after stress release (see Rehschuh et al. 2021). During the second half of the recovery period, growth rates exceeded those of the control seedlings largely independent of net C uptake ($P < 0.05$; Figure 2c).

Stress impairment and delayed recovery

Because the degree of evaporative cooling from transpiration differed among treatments, seedlings exposed to combined heat

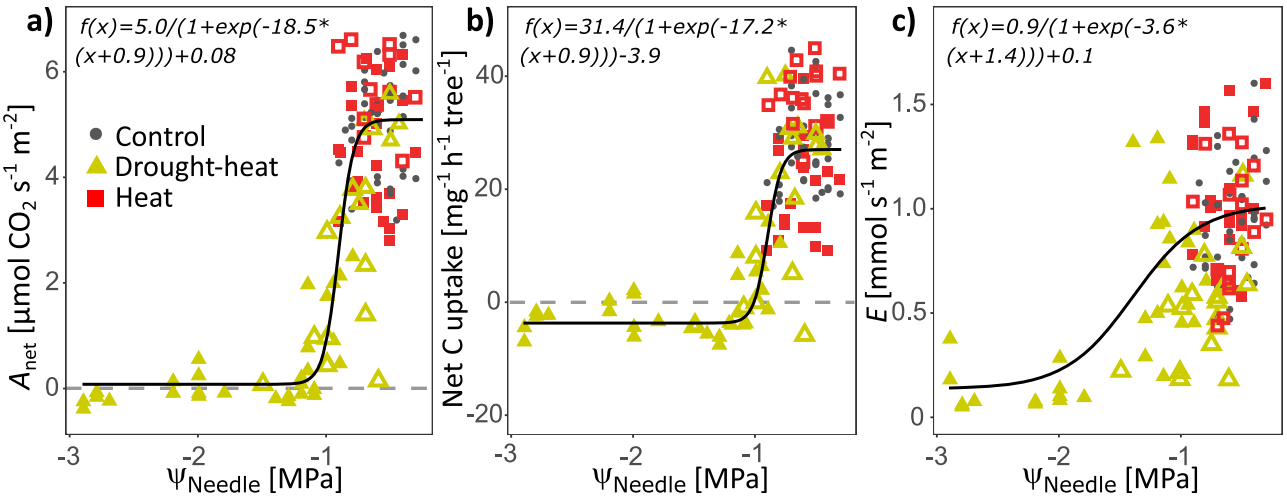

Figure 6. Dependencies of (a) net assimilation (A_{net}), (b) net C uptake, and (c) transpiration (E) with needle water potential (Ψ_{Needle}) measured at noon during stress and recovery. Each data point shows a measurement per seedling. The different treatments are highlighted and open symbols indicate measurements during the recovery period. Sigmoidal functions were fitted to drought-heat (excluding recovery) and control measurements. Root-mean-square error: A_{net}: 0.86; net C uptake: 6.15; E: 0.30.

and drought experienced substantially (3–4.5 °C) higher leaf temperatures than seedlings of the heat treatment (Figure 3a, Figure S9 available as Supplementary data at *Tree Physiology* Online). Leaf temperatures were significantly higher compared with the control in both stress treatments, whereas in the heat treatment evaporative cooling maintained mean leaf temperature below maximum T_{air}.

The effect of high leaf temperatures was also apparent in the decline of A_{net} and simultaneous decrease in photosystem II activity (here F'_v/F'_m; Figure 3e and f). Albeit F'_v/F'_m was not affected by the initial drought, it decreased strongly within the course of the heatwave, reaching 80% lower values than the control ($P < 0.05$; Figure 3b). Seedlings in the heat treatment were less affected, but F'_v/F'_m also decreased by 30% compared with the control ($P < 0.05$). These effects were fully reversed within the recovery period in both stress treatments, with a delay in drought-heat seedlings. Although the relationship between A_{net} and leaf temperature differed between the heat and drought-heat treatment (including recovery), F'_v/F'_m showed a rather similar leaf temperature response pattern in both stress treatments (Figure 3f). In contrast to pronounced stress effects on photosystem II, we found no apparent needle cell damage in heat and drought-heat seedlings. Electrolyte leakage only tended to be increased on Day 23 when highest leaf temperatures were reached, but did not differ significantly from the control (Figure 3c and g).

Further, hydraulic parameters were affected mildly under heat, but strongly under drought-heat. K_{Leaf} was reduced during the initial drought period, and continued to decline with heat initiation in both stress treatments (Figure 3d), reaching c. 90% lower values in the drought-heat treatment compared with the control ($P < 0.05$). This decline was partially associated with high leaf temperatures (Figure 3h). Although the other stress-related parameters recovered fully, K_{Leaf} did not reach control values in drought-heat treated seedlings until the end of the experiment ($P < 0.05$). Similarly, K_S was c. 25% lower post drought-heat compared with the control 18 days after stress release, indicating that K_S did not recover ($P < 0.05$, Figure 4a and b). However, the stress impacts were less apparent than for K_{Leaf} (Figure 4c).

Drought-heat stress had large impacts on Ψ_{Needle}, which decreased to min. −2.70 ± 0.13 MPa ($P < 0.05$, Figure 5a). Although heat stress alone did not affect Ψ_{Needle}, RWC_{Needle} was slightly lower in the heat treatment compared with the control during the hottest days (Figure 5b). In the drought-heat treatment, the decline in RWC_{Needle} was more pronounced and appeared earlier during the experiment. Ψ_{Needle} and RWC_{Needle} recovered to control values nearly immediately following stress release.

Further, a close relationship of A_{net}, net C uptake and E with Ψ_{Needle} was apparent in the drought-heat treatment (Figure 6). A_{net} halted or turned negative (i.e., shoot respiration and photorespiration exceeded assimilation) at a Ψ_{Needle} of c. −1.16 MPa, while the tree net C uptake turned negative slightly earlier at a Ψ_{Needle} of c. −1.08 MPa. This indicates a dominant role of tree hydraulic processes in limiting gas exchange rates during hot droughts. The recovery of these gas exchange parameters appeared to largely follow the increase in Ψ_{Needle}, with a tendency of slightly lower E post-drought-heat.

Discussion

We closely monitored stress and recovery responses of Scots pine seedlings exposed to heat or drought-heat stress. All

seedlings successfully survived the heatwave, while additional drought delayed recovery as observed in photosynthetic and hydraulic responses. Moreover, we found all seedlings to recover daily net C uptake quickly, indicating that a new equilibrium at the tree level between C uptake and release appeared largely independent of persisting hydraulic impairment.

Thermal stress but no needle damage

A gradually increasing heatwave over 20 days resulted in daytime temperatures above 35 °C on 14 days with 40 °C reached on 3 days. Heat stress alone affected the hydraulic system moderately, but in combination with drought, stress impacts intensified. Both, on a diurnal scale and in the course of the heatwave, we found E to increase with rising T_{air} in the well-watered heat treatment (Figure 1f; Ameye et al. 2012, Ruehr et al. 2016). Under water-limiting conditions and high VPD in the drought-heat treatment, E decreased strongly during the second half of the day to prevent extensive water loss and high xylem tensions, alongside declining g_s (Figure S5 available as Supplementary data at *Tree Physiology* Online; Zhao et al. 2013, Ruehr et al. 2016, Birami et al. 2018). This is in contrast to Urban et al. (2017*b*, 2017*a*), who found g_s to increase with rising temperatures, even under low VWC. Stomatal adjustment affects evaporative cooling of transpiring leaves, thus decreasing leaf temperatures. In our study, seedlings of the heat treatment were able to keep leaf temperatures below maximum T_{air} (Figure 3a), as E increased despite declining g_s. Under drought-heat, the limited capacity of needle cooling due to reduced E resulted in higher leaf temperatures (max. 46 °C) during early afternoon. Although tree mortality has been reported following hot drought stress (Allen et al. 2010, Balducci et al. 2013, Teskey et al. 2015) and leaf temperatures similar to our study (47 °C in Birami et al. (2018)), we did not find negative effects on seedling survival nor direct tissue damage. This was supported by negligible electrolyte leakage in tissues of completely matured needles (Figure 3c and g). Similar temperatures would supposedly have been more damaging in developing, not hardened tissues (Ruehr et al. 2016). Partially, this might have also been prevented by relatively high E rates during early mornings in drought-heat seedlings, buffering some of the excessive needle temperature stress. Moreover, the duration of the temperature exposure is important. In our study, the heatwave resulted in a total of 18 h at c. 40 °C T_{air}. However, in well-watered seedlings of *Pinus radiata* at T_{air} and heat exposure comparable to our study, significant increases in electrolyte leakage were observed (Escandón et al. 2016). The discrepancy might result from the gradual increase of temperatures in our study compared with the immediate temperature increment from 25 to 40 °C in Escandón et al. (2016), allowing the seedlings to acclimate cell membrane stability to thermal stress (Saelim and Zwiazek 2000).

Although it is difficult to clearly disentangle the impacts of high temperatures on our drought treatment, needle damage was not obvious albeit the very high leaf temperatures during periods of low transpiration during early afternoon. Hence, we found a remarkable thermal resistance of fully matured Scots pine needles to temperatures of 46 °C for several hours and have to partially reject our first hypothesis.

Tree hydraulics during stress and recovery

Both, the heat and drought-heat treatment affected K_{Leaf} (Figure 3d). In response to heat alone, the decline was modest and might be related to the high temperatures and increases in VPD. Most likely, the decline of K_{Leaf} in the heat treatment originated from impacts on extra-xylary tissues as observed by a moderate decline of RWC_{Needle}. The underlying mechanism might be shrinkage of cells and tissues and/or the reduction in aquaporin activity (Cochard et al. 2004, Sack et al. 2016, Scoffoni et al. 2014). In the drought-heat treatment, K_{Leaf} declined further alongside larger reductions in Ψ_{Needle}, indicating that leaf xylem embolism appeared later during stress progression (Brodribb and Cochard 2009, Johnson et al. 2009, Lo Gullo et al. 2005). The minimum Ψ_{Needle} indicated mild degrees of stem xylem embolism, i.e., 27% loss of hydraulic conductivity (PLC) as derived from hydraulic vulnerability curves (Rehschuh et al. 2020). This refers well to the measured reduction of K_S by 25% in drought-heat compared with control seedlings at the end of the experiment (Figure 4a and b). Based thereon, we suggest embolism as underlying reason for the incomplete recovery of K_{Leaf} within the 18-day recovery period (Figure 4c). If solely extra-xylary tissues had been affected, we could assume K_{Leaf} to recover faster alongside RWC_{Needle} and Ψ_{Needle} (Brodribb and Cochard 2009, Laur and Hacke 2014) due to rehydration not related to refilling of xylem embolism. In agreement, in heat seedlings, we observed a fast recovery of RWC_{Needle} and K_{Leaf}, supported by full K_S integrity (Figure 4a and b). This agrees with a recent stress-recovery framework by Ruehr et al. (2019), indicating that xylem embolism delays hydraulic recovery, while extra-xylary conductance can be recovered quickly. Additionally, the stronger reduction of K_{Leaf} than K_S in response to water limitation (Figure 4b and c) indicates the higher vulnerability of distal organs such as leaves compared with stems (Bartlett et al. 2016, Brodribb and Cochard 2009) in hydraulically segmented Scots pine.

Overall, we show that during a modest but prolonged heatwave the impact on the hydraulic system became substantial when combined with drought, resulting in persisting reductions of conductivity in needle and stem tissues.

Metabolic responses during stress and recovery

The stress imposed by high temperatures was further reflected in the C metabolism of the seedlings. During heatwave progression, A_{net} declined moderately in response to higher leaf

temperatures (c. 40 °C) in the heat treatment (Figure 1e and 3e; Bernacchi et al. 2002, Birami et al. 2020), and the decrease in g_s (Figure S5 available as Supplementary data at *Tree Physiology* Online) helped to maintain high Ψ_{Needle} in these isohydric pines (Figure 6a). In contrast, in the drought-heat treatment, A_{net} decreased strongly with stress progression and declining Ψ_{Needle} (Figure 6a), concurrently with a heavy decline in g_s (Figure S6 available as Supplementary data at *Tree Physiology* Online; Ruehr et al. 2016; Birami et al. 2018). A_{net} was modulated by a strong diurnal pattern in both stress treatments with larger C uptake during the cooler morning hours, directly after irrigation (Bauweraerts et al. 2013, Drake et al. 2018). The decline in A_{net} was accompanied by a decrease in F'_v/F'_m in the heat treatment (Ameye et al. 2012, Guha et al. 2018) and with a more severe reduction in drought-heat seedlings (Figure 3b; Birami et al. 2018). Additional chlorophyll fluorescence parameters, such as electron transfer rate, effective photosystem II quantum yield and coefficients of photochemical fluorescence quenching, have been shown to reveal strong decreases under heat and drought stress (Ameye et al. 2012, Birami et al. 2018). F'_v/F'_m serves to assess stress impacts of the photosynthetic apparatus (Netto et al. 2005). Its decrease can be seen as a protective mechanism, which eliminates excess excitation energy, thus inhibiting the formation of harmful free radicals (Murchie and Lawson 2013). The observed fast recovery of F'_v/F'_m in the heat treatment is in line with previous studies (Ameye et al. 2012, Birami et al. 2018, Guha et al. 2018), while the full recovery was delayed in drought-heat seedlings. Toward the end of the experimental recovery period, F'_v/F'_m had fully recovered and A_{net} reached 80% of control rates. This indicates that neither single nor compound stress had substantially harmed the photosynthetic apparatus.

Regarding R_{root}, we found at first an increase with rising temperatures in the heat treatment (Figure 1g, Figures S7 and S8 available as Supplementary data at *Tree Physiology* Online) as commonly observed (Birami et al. 2020, Burton et al. 2002, Jarvi and Burton 2013). The subsequent observed decline at $T_{soil} > 34$ °C is in agreement with a study on Aleppo pine seedlings, where R_{root} peaked at 31–34 °C (Birami et al. 2020). This might indicate a respiratory acclimation response as shown also in other studies (e.g., Jarvi and Burton 2013). In drought-heat seedlings, R_{root} decreased strongly with drought progression and was insensitive to temperature changes (Figure S7 available as Supplementary data at *Tree Physiology* Online). Explanations for the decline in respiration might be growth cessation, reduced assimilates, and at the cellular level limitation of available C as substrate and/or adenylate control (Atkin and Tjoelker 2003, Birami et al. 2020, Dusenge et al. 2019, O'Leary et al. 2019). Further, decreased C transport to sink organs might play a role during drought (Blessing et al. 2015, Ruehr et al. 2009). Despite reduced R_{root} under drought-heat, the whole-tree C balance became negative, which was dominated by a strong decline in A_{net} (Figure 2a, Figure S8 available as Supplementary data at *Tree Physiology* Online; Zhao et al. 2013), with A_{net} and C uptake halting or turning negative at a Ψ_{Needle} of c. −1.0 MPa (Figure 6a and b).

Following release from heat stress in the heat treatment, the full recovery of shoot gas exchange is in agreement with a fully functional stem xylem (Figure 4a and b). In contrast, delayed recovery of A_{net} in the drought-heat treatment post-stress might be related to persisting reductions of K_{Leaf} and K_S (Brodribb and Cochard 2009, Rehschuh et al. 2020, Skelton et al. 2017). R_{root} of drought-heat seedlings initially increased slowly during recovery and C allocation to belowground was delayed (Rehschuh et al. 2021), but finally surpassed control rates at the end of the 18-day recovery period (Figure 1g). This indicates enhanced belowground repair mechanisms and root development to reestablish a fully functional root system (Davidson et al. 2006, Hagedorn et al. 2016) later during recovery.

Overall, we show that the C metabolism was affected moderately in heat but strongly in drought-heat seedlings. The decline of F'_v/F'_m in both treatments indicates a protective mechanism of the photosynthetic apparatus, and its full recovery points toward no persistent photosynthetic damage. Alongside, A_{net} and respiration rates recovered almost fully, indicating a relatively fast restoration of the seedlings' C metabolism. This largely confirms our second hypothesis.

Coupling of net C uptake and stem diameter change during stress and recovery

Stress-induced changes in water cycling and net C uptake simultaneously affected stem diameter change (Figure 2). Note that the growing season was prolonged under controlled conditions with daytime length of 16 h and favorable temperatures (26 °C/15 °C day/night) that allowed stem growth to continue throughout the experiment in control seedlings. This contrasts with growth cessation of *P. sylvestris* under field conditions earlier in the year (e.g., Michelot et al. 2012). During the heatwave, stem growth (i.e., cell division and/or cell elongation) ceased in drought-heat seedlings as cambium activity typically decreases at high xylem tension and low turgor (Abe et al. 2003, Balducci et al. 2013, 2016, Deslauriers et al. 2014), in agreement with the negative daily C balance (Figure 2b). Further, stem shrinkage can be related to increased tree water deficit in phloem and xylem tissues (Zweifel et al. 2000). In the heat treatment, the positive but reduced daily net C balance apparently had less influence on stem growth rates than reported elsewhere (Bauweraerts et al. 2014, Ruehr et al. 2016). Following heat release, we observed an increase in stem growth rates above control rates alongside a slight overcompensation of A_{net} and associated higher daily net C balance (Figures 1e and 2). Moreover, we found recent C to be allocated quickly to branch cellulose

(see Rehschuh et al. 2021). This suggests stress compensatory responses (Balducci et al. 2016, Ruehr et al. 2016).

Interestingly, in drought-heat seedlings, in which leaf-level A_{net} remained largely below control rates while tissue-specific R_{root} recovered, tree net C uptake regained control rates quickly, i.e., 2 days after stress release. This could reflect a relatively lower sink demand, as root biomass and the root:shoot ratio tended to be lower in drought-heat seedlings. Hence, the fast recovery of net C uptake might suggest that the seedlings rebalanced C uptake and release, largely independent of the reduced recovery of hydraulic conductance. Thus, we suggest that persistently lower K_S and K_{Leaf} in drought-heat seedlings did not translate into limitations of A_{net} and E under the generally low VPD conditions during the recovery period. During times of low VPD, the hydraulic system is operating far away from its maximum capacity, hence relatively small reductions in conductance as observed here should have little effect on the water transport system and hence C uptake. In agreement, environmental conditions during recovery are an important factor to consider when drawing conclusions on the underlying mechanisms of stress legacy. However, if another heat event occurs before the hydraulic system is fully restored, the persisting reductions of K_S and K_{Leaf} as observed here should limit E more strongly, thus reducing evaporative cooling and increasing thermal stress.

Therefore, enhanced stem growth rates in recovering drought-heat seedlings as observed during the second week of recovery support a preference for the restoration of maximum hydraulic conductivity in the long-term (Balducci et al. 2013, Brodribb and Cochard 2009).

Opposing to our third hypothesis, this indicates a relatively fast regulation of the tree net C balance, appearing to be independent of hydraulic impairment under the recovery conditions applied here. However, we assume that enhanced stem growth post- drought-heat may support the repair of the hydraulic system in the long term to restore maximum K_S and increase the resistance to future stress conditions.

Conclusion

Our study demonstrated that heat in combination with drought amplified the impacts on the C and water balance of Scots pine seedlings compared with heat stress alone. We did not observe temperature-induced damage of mature needles, while impacts on developing needles earlier during the season could potentially be more severe. Seedlings of the heat treatment were able to mitigate temperature stress by sustained evaporative cooling, while g_s and A_{net} declined moderately. This was also reflected in post-stress dynamics, indicating a fast recovery once heat stress was released. In contrast, we found a delayed recovery of R_{root} and A_{net} in the drought-heat treatment, while the photosynthetic apparatus appeared undamaged albeit high temperatures. Nonetheless, the daily net C balance in drought-heat seedlings recovered within 2 days after stress release, suggesting a new equilibrium between C uptake and release. This was largely independent of the delayed recovery of K_{Leaf} and K_S, which most likely did not affect the C balance because the water transport system operated far away from its maximum capacity during the recovery conditions applied here. Stem growth was upregulated during the second week of recovery, potentially contributing to the repair of the hydraulic system in the long-term. Although our study shows that Scots pine seedlings are able to survive leaf temperatures of 46 °C alongside late seasonal drought, it also indicates that they might be vulnerable to subsequent stress periods as the integrity of the hydraulic system and supporting biomass were not fully restored yet. This might be particularly critical following early season stress, when trees are limited by the time available to fully recover before another heatwave strikes.

Supplementary data

Supplementary data for this article are available at *Tree Physiology* Online.

Acknowledgments

We would like to thank Andreas Gast, Andrea Jakab, Benjamin Birami, Marielle Gattmann, Barbara Beikircher and Stefan Mayr for technical and experimental support and advice. This study was supported by the German Research Foundation through its Emmy Noether Program (RU 1657/2-1) and by the German Federal Ministry of Education and Research (BMBF) through the Helmholtz Association and its research program ATMO.

Authors' contributions

R.R. and N.K.R. designed the study. R.R. conducted the experiment and analyzed the data with support from N.K.R. R.R. wrote the original draft, with reviewing and editing from N.K.R.

Conflict of interest

None declared.

Data and materials availability

Data that support the findings of this study will be made available upon request.

References

Abe H, Nakai T, Utsumi Y, Kagawa A (2003) Temporal water deficit and wood formation in Cryptomeria japonica. Tree Physiol 23:859–863.

Allen CD, Macalady AK, Chenchouni H et al. (2010) A global overview of drought and heat-induced tree mortality reveals emerging climate change risks for forests. For Ecol Manage 259:660–684.

Ameye M, Wertin TM, Bauweraerts I, McGuire MA, Teskey RO, Steppe K (2012) The effect of induced heat waves on *Pinus taeda* and *Quercus rubra* seedlings in ambient and elevated CO_2 atmospheres. New Phytol 196:448–461.

Anderegg WRL, Schwalm C, Biondi F et al. (2015) Pervasive drought legacies in forest ecosystems and their implications for carbon cycle models. Science 349:528–532.

Anderegg WRL, Anderegg LDL, Kerr KL, Trugman AT (2019) Widespread drought-induced tree mortality at dry range edges indicates that climate stress exceeds species' compensating mechanisms. Glob Chang Biol 25:3793–3802.

Arend M, Link RM, Patthey R, Hoch G, Schuldt B, Kahmen A (2021) Rapid hydraulic collapse as cause of drought-induced mortality in conifers. Proc Natl Acad Sci USA 118:e2025251118. https://doi.org/10.1073/pnas.2025251118.

Atkin OK, Tjoelker MG (2003) Thermal acclimation and the dynamic response of plant respiration to temperature. Trends Plant Sci 8:343–351.

Atkin OK, Edwards EJ, Loveys BR (2000) Response of root respiration to changes in temperature and its relevance to global warming. New Phytol 147:141–154.

Balducci L, Deslauriers A, Giovannelli A, Rossi S, Rathgeber CBK (2013) Effects of temperature and water deficit on cambial activity and woody ring features in *Picea mariana* saplings. Tree Physiol 33:1006–1017.

Balducci L, Cuny HE, Rathgeber CBK, Deslauriers A, Giovannelli A, Rossi S (2016) Compensatory mechanisms mitigate the effect of warming and drought on wood formation. Plant Cell Environ 39:1338–1352.

Bartlett MK, Klein T, Jansen S, Choat B, Sack L (2016) The correlations and sequence of plant stomatal, hydraulic, and wilting responses to drought. Proc Natl Acad Sci USA 113:13098–13103.

Bauweraerts I, Wertin TM, Ameye M, McGuire MA, Teskey RO, Steppe K (2013) The effect of heat waves, elevated [CO_2] and low soil water availability on northern red oak (*Quercus rubra* L.) seedlings. Glob Chang Biol 19:517–528.

Bauweraerts I, Ameye M, Wertin TM, McGuire MA, Teskey RO, Steppe K (2014) Water availability is the decisive factor for the growth of two tree species in the occurrence of consecutive heat waves. Agric For Meteorol 189–190:19–29.

Bernacchi CJ, Portis AR, Nakano H (2002) Temperature response of mesophyll conductance. Implications for the determination of rubisco enzyme kinetics and for limitations to photosynthesis in vivo. Plant Physiol 130:1992–1998.

Birami B, Gattmann M, Heyer AG, Grote R, Arneth A, Ruehr NK (2018) Heat waves alter carbon allocation and increase mortality of Aleppo pine under dry conditions. Front Forests Global Change 1:8. https://doi.org/10.3389/ffgc.2018.00008.

Birami B, Nägele T, Gattmann M, Preisler Y, Gast A, Arneth A, Ruehr NK (2020) Hot drought reduces the effects of elevated CO_2 on tree water-use efficiency and carbon metabolism. New Phytol 226:1607–1621..

Blessing CH, Werner RA, Siegwolf R, Buchmann N (2015) Allocation dynamics of recently fixed carbon in beech saplings in response to increased temperatures and drought. Tree Physiol 35:585–598.

Brodribb TJ, Cochard H (2009) Hydraulic failure defines the recovery and point of death in water-stressed conifers. Plant Physiol 149:575–584.

Brodribb TJ, Bowman DJMS, Nichols S, Delzon S, Burlett R (2010) Xylem function and growth rate interact to determine recovery rates after exposure to extreme water deficit. New Phytol 188:533–542.

Burnham K, Anderson D (2002) Model selection and multi-model inference. Springer, New York, NY.

Burton AJ, Pregitzer KS, Ruess RW, Hendrick RL, Allen MF (2002) Root respiration in north American forests: effects of nitrogen concentration and temperature across biomes. Oecologia 131:559–568.

Ciais P, Reichstein M, Viovy N et al. (2005) Europe-wide reduction in primary productivity caused by the heat and drought in 2003. Nature 437:529–533.

Cochard H, Froux F, Mayr S, Coutand C (2004) Xylem wall collapse in water-stressed pine needles. Plant Physiol 134:401–408.

Correia B, Valledor L, Meijón M, Rodriguez JL, Dias MC, Santos C, Cañal MJ, Rodriguez R, Pinto G (2013) Is the interplay between epigenetic markers related to the acclimation of Cork oak plants to high temperatures? PLoS One 8:e53543. https://doi.org/10.1371/journal.pone.0053543.

Davidson EA, Janssens IA, Luo Y (2006) On the variability of respiration in terrestrial ecosystems: moving beyond Q_{10}. Glob Chang Biol 12:154–164.

De Boeck HJ, Dreesen FE, Janssens IA, Nijs I (2010) Climatic characteristics of heat waves and their simulation in plant experiments. Glob Chang Biol 16:1992–2000.

Demidchik V, Straltsova D, Medvedev SS, Pozhvanov GA, Sokolik A, Yurin V (2014) Stress-induced electrolyte leakage: the role of K+-permeable channels and involvement in programmed cell death and metabolic adjustment. J Exp Bot 65:1259–1270.

Deslauriers A, Beaulieu M, Balducci L, Giovannelli A, Gagnon MJ, Rossi S (2014) Impact of warming and drought on carbon balance related to wood formation in black spruce. Annals of Botany 114:335–345.

Drake JE, Tjoelker MG, Medlyn BE et al. (2018) Trees tolerate an extreme heatwave via sustained transpirational cooling and increased leaf thermal tolerance. Glob Chang Biol 24:2390–2402.

Duarte AG, Katata G, Hoshika Y, Hossain M, Kreuzwieser J, Arneth A, Ruehr NK (2016) Immediate and potential long-term effects of consecutive heat waves on the photosynthetic performance and water balance in Douglas-fir. J Plant Physiol 205:57–66.

Dusenge ME, Duarte AG, Way DA (2019) Plant carbon metabolism and climate change: elevated CO_2 and temperature impacts on photosynthesis, photorespiration and respiration. New Phytol 221:32–49.

Ellenberg H, Leuschner C (2010) Vegetation Mitteleuropas mit den Alpen: in ökologischer, dynamischer und historischer Sicht, Vol. 8104, ed. Utb. Stuttgart: Ulmer Verlag.

Escandón M, Cañal MJ, Pascual J, Pinto G, Correia B, Amaral J, Meijón M (2016) Integrated physiological and hormonal profile of heat-induced thermotolerance in *Pinus radiata*. Tree Physiol 36:63–77.

Galiano L, Martínez-Vilalta J, Lloret F (2011) Carbon reserves and canopy defoliation determine the recovery of Scots pine 4 yr after a drought episode. New Phytol 190:750–759.

Gauthier PPG, Crous KY, Ayub G, et al. (2014) Drought increases heat tolerance of leaf respiration in *Eucalyptus globulus* saplings grown under both ambient and elevated atmospheric [CO_2] and temperature. J Exp Bot 65:6471–6485.

Größwein S, Lemme H, Buras A, Schunk C, Menzel A, Straub C, Mette T, Taeger S (2017) Kiefernschäden in Bayern. LWF Aktuell 112:12–13.

Grossiord C, Buckley TN, Cernusak LA, Novick KA, Poulter B, Siegwolf RTW, Sperry JS, McDowell NG (2020) Plant responses to rising vapor pressure deficit. New Phytol 226:1550–1566.

Guha A, Han J, Cummings C, McLennan DA, Warren JM (2018) Differential ecophysiological responses and resilience to heat wave events in four co-occurring temperate tree species. Environ Res Lett 13:065008.

Hagedorn F, Joseph J, Peter M et al. (2016) Recovery of trees from drought depends on belowground sink control. Nat Plants 2:1–5.

Hanewinkel M, Cullmann DA, Schelhaas M-J, Nabuurs G-J, Zimmermann NE (2013) Climate change may cause severe loss in the economic value of European forest land. Nat Clim Change 3:203–207.

Ionita M, Tallaksen LM, Kingston DG, Stagge JH, Laaha G, Van Lanen HAJ, Scholz P, Chelcea SM, Haslinger K (2017) The European 2015 drought from a climatological perspective. Hydrol Earth Syst Sci 21:1397–1419.

IPCC (2018) Summary for policymakers. In: Global Warming of 1.5 °C. https://www.ipcc.ch/sr15/chapter/spm/.

Jarvi MP, Burton AJ (2013) Acclimation and soil moisture constrain sugar maple root respiration in experimentally warmed soil. Tree Physiol 33:949–959.

Johnson DM, Meinzer FC, Woodruff DR, Mcculloh KA (2009) Leaf xylem embolism, detected acoustically and by cryo-SEM, corresponds to decreases in leaf hydraulic conductance in four evergreen species. Plant Cell Environ 32:828–836.

Kumarathunge DP, Drake JE, Tjoelker MG, López R, Pfautsch S, Vårhammar A, Medlyn BE (2020) The temperature optima for tree seedling photosynthesis and growth depend on water inputs. Glob Chang Biol 26:2544–2560.

Kunert N (2020) Preliminary indications for diverging heat and drought sensitivities in Norway spruce and Scots pine in central. Europe iForest 13:89–91.

Kuznetsova A, Brockhoff PB, Christensen RHB (2017) lmerTest package: tests in linear mixed effects models. J Stat Softw 82:1–26..

Larkindale J, Knight MR (2002) Protection against heat stress-induced oxidative damage in Arabidopsis involves calcium, abscisic acid, ethylene, and salicylic acid. Plant Physiol 128:682–695.

Laur J, Hacke UG (2014) Exploring *Picea glauca* aquaporins in the context of needle water uptake and xylem refilling. New Phytol 203:388–400.

Lenth R, Singmann H, Love J, Buerkner P, Herve M (2020) Emmeans: estimated marginal means, aka least-squares means. https://github.com/rvlenth/emmeans.

Lo Gullo MA, Nardini A, Trifilo P, Salleo S (2005) Diurnal and seasonal variations in leaf hydraulic conductance in evergreen and deciduous trees. Tree Physiol 25:505–512.

McDowell NG, Allen CD, Anderson-Teixeira K et al. (2020) Pervasive shifts in forest dynamics in a changing world. Science 368:eaaz9463.

Mena-Petite A, Robredo A, Alcalde S, Duñabeitia M, González-Moro M, Lacuesta M, Muñoz-Rueda A (2003) Gas exchange and chlorophyll fluorescence responses of *Pinus radiata* D. Don seedlings during and after several storage regimes and their effects on post-planting survival. Trees 17:133–143.

Michelot A, Simard S, Rathgeber C, Dufrêne E, Damesin C (2012) Comparing the intra-annual wood formation of three European species (*Fagus sylvatica*, *Quercus petraea* and *Pinus sylvestris*) as related to leaf phenology and non-structural carbohydrate dynamics. Tree Physiol 32:1033–1045.

Murchie EH, Lawson T (2013) Chlorophyll fluorescence analysis: a guide to good practice and understanding some new applications. J Exp Bot 64:3983–3998.

Netto AT, Campostrini E, de Oliveira JG, Bressan-Smith RE (2005) Photosynthetic pigments, nitrogen, chlorophyll a fluorescence and SPAD-502 readings in coffee leaves. Sci Hortic 104:199–209.

O'Kane D, Gill V, Boyd P, Burdon R (1996) Chilling, oxidative stress and antioxidant responses in *Arabidopsis thaliana callus*. Planta 198: 371–377.

O'Leary BM, Asao S, Millar AH, Atkin OK (2019) Core principles which explain variation in respiration across biological scales. New Phytol 222:670–686.

R Development Core Team (2019) R: A language and environment for statistical computing. R Foundation for Statistical Computing, Vienna, Austria.

Rehschuh R, Mette T, Menzel A, Buras A (2017) Soil properties affect the drought susceptibility of Norway spruce. Dendrochronologia 45:81–89.

Rehschuh R, Cecilia A, Zuber M, Faragó T, Baumbach T, Hartmann H, Jansen S, Mayr S, Ruehr N (2020) Drought-induced xylem embolism limits the recovery of leaf gas exchange in Scots pine. Plant Physiol 184:852–864.

Rehschuh R, Rehschuh S, Gast A, Jakab A, Lehmann M, Saurer M, Gessler A, Ruehr NK (2021) Tree allocation dynamics beyond heat and hot drought stress reveal changes in carbon storage, belowground translocation and growth. New Phytol. https://doi.org/10.1111/nph.17815.

Ruehr NK, Gast A, Weber C, Daub B, Arneth A (2016) Water availability as dominant control of heat stress responses in two contrasting tree species. Tree Physiol 36:164–178.

Ruehr NK, Offermann CA, Gessler A, Winkler JB, Ferrio JP, Buchmann N, Barnard RL (2009) Drought effects on allocation of recent carbon: from beech leaves to soil CO_2 efflux. New Phytol 184:950–961.

Ruehr NK, Grote R, Mayr S, Arneth A (2019) Beyond the extreme: recovery of carbon and water relations in woody plants following heat and drought stress. Tree Physiol 39:1285–1299.

Sack L, Scoffoni C (2012) Measurement of leaf hydraulic conductance and stomatal conductance and their responses to irradiance and dehydration using the Evaporative Flux Method (EFM). J Vis Exp 70:e4179. https://doi.org/10.3791/4179.

Sack L, Buckley TN, Scoffoni C (2016) Why are leaves hydraulically vulnerable? J Exp Bot 67:4917–4919.

Saelim S, Zwiazek JJ (2000) Preservation of thermal stability of cell membranes and gas exchange in high temperature acclimated *Xylia xylocarpa* seedlings. J Plant Physiol 156:380–385.

Sage RF, Way DA, Kubien DS (2008) Rubisco, rubisco activase, and global climate change. J Exp Bot 59:1581–1595.

Scherrer D, Bader MK-F, Körner C (2011) Drought-sensitivity ranking of deciduous tree species based on thermal imaging of forest canopies. Agric For Meteorol 151:1632–1640.

Schrader SM, Wise RR, Wacholtz WF, Ort DR, Sharkey TD (2004) Thylakoid membrane responses to moderately high leaf temperature in Pima cotton. Plant Cell Environ 27:725–735.

Schuldt B, Buras A, Arend M et al. (2020) A first assessment of the impact of the extreme 2018 summer drought on central European forests. Basic Appl Ecol 45:86–103.

Scoffoni C, Vuong C, Diep S, Cochard H, Sack L (2014) Leaf shrinkage with dehydration: coordination with hydraulic vulnerability and drought tolerance. Plant Physiol 164:1772–1788.

Sellin A, Kupper P (2007) Temperature, light and leaf hydraulic conductance of little-leaf linden (*Tilia cordata*) in a mixed forest canopy. Tree Physiol 27:679–688.

Skelton RP, Brodribb TJ, McAdam SAM, Mitchell PJ (2017) Gas exchange recovery following natural drought is rapid unless limited by loss of leaf hydraulic conductance: evidence from an evergreen woodland. New Phytol 215:1399–1412.

Smith AM, Stitt M (2007) Coordination of carbon supply and plant growth. Plant Cell Environ 30:1126–1149.

Sperry JS, Tyree MT (1988) Mechanism of water stress-induced xylem embolism. Plant Physiol 88:581–587.

Teskey R, Wertin T, Bauweraerts I, Ameye M, Mcguire MA, Steppe K (2015) Responses of tree species to heat waves and extreme heat events: tree response to extreme heat. Plant Cell Environ 38:1699–1712.

Urban J, Ingwers M, McGuire MA, Teskey R (2017*a*) Stomatal conductance increases with rising temperature. Plant Signal Behav 12:e1356534.

Urban J, Ingwers MW, McGuire MA, Teskey RO (2017*b*) Increase in leaf temperature opens stomata and decouples net photosynthesis from

stomatal conductance in *Pinus taeda* and *Populus deltoides x nigra*. J Exp Bot 68:1757–1767.

von Caemmerer S, Evans JR (2015) Temperature responses of mesophyll conductance differ greatly between species: temperature responses of mesophyll conductance. Plant Cell Environ 38:629–637.

Walentowski H, Falk W, Mette T, Kunz J, Bräuning A, Meinardus C, Zang C, Sutcliffe LME, Leuschner C (2017) Assessing future suitability of tree species under climate change by multiple methods: a case study in southern Germany. Ann For Res 60:101–126.

Way DA, Domec J-C, Jackson RB (2013) Elevated growth temperatures alter hydraulic characteristics in trembling aspen (*Populus tremuloides*) seedlings: implications for tree drought tolerance. Plant Cell Environ 36:103–115.

Zhao J, Hartmann H, Trumbore S, Ziegler W, Zhang Y (2013) High temperature causes negative whole-plant carbon balance under mild drought. New Phytol 200:330–339.

Zweifel R, Häsler R (2000) Frost-induced reversible shrinkage of bark of mature subalpine conifers. Agric For Meteorol 102: 213–222.

Zweifel R, Item H, Häsler R (2000) Stem radius changes and their relation to stored water in stems of young Norway spruce trees. Trees 15:50–57.